J Mater Sci (2011) 46:2018–2023
DOI 10.1007/s10853-010-4851-3

Optical properties of Dy^{3+}-doped sodium–aluminum–phosphate glasses

**A. Amarnath Reddy · M. Chandra Sekhar ·
K. Pradeesh · S. Surendra Babu · G. Vijaya Prakash**

Received: 18 May 2010 / Accepted: 19 August 2010 / Published online: 14 January 2011

Abstract Trivalent dysprosium (Dy^{3+})-doped sodium–aluminum–phosphate (NAP) glasses were prepared and characterized by their optical absorption, excitation, emission spectra, and decay time measurements. Judd–Ofelt intensity parameters were derived from the absorption spectrum and used to calculate the radiative lifetime and stimulated emission cross section of the $^4F_{9/2} \rightarrow {}^6H_{13/2}$ and $^4F_{9/2} \rightarrow {}^6H_{15/2}$ transitions. The luminescence intensity ratio of $^4F_{9/2} \rightarrow {}^6H_{13/2}$ to $^4F_{9/2} \rightarrow {}^6H_{15/2}$ transitions of Dy^{3+} in NAP glasses gives the feasibility of extracting white light. The lifetime and quantum efficiency of $^4F_{9/2}$ level is found to be higher than other reported glasses. With increase in Dy^{3+} ion concentration, the decay from $^4F_{9/2}$ level is found to be faster with decrease in lifetime due to cross relaxation between Dy^{3+} ions.

Introduction

Recent progress in the development of special photonic glasses is reshaping the laser industry by pushing rare earth (RE)-based waveguide/fiber lasers to the forefront of solid-state laser applications. However, the choice of appropriate glass matrix, for low-cost and compact planar waveguides, with larger amount of RE ions is still a formidable task [1–4]. Among different glass hosts such as silicate, borate, etc., phosphate glasses have their unique characteristics that include high thermal stability, high transparency, low-melting point, high gain density that is due to high solubility for RE ions and low dispersion [5–8]. Introduction of Al_2O_3 into phosphate glass network well increases the cross-linking between PO_4 tetrahedra in the glass which results in moisture free and thermally stable glass with low thermal coefficient of expansion that are used for ion-exchange planar waveguide devices [5, 9, 10]. Also the presence of Na_2O improves the RE ion solubility leading to the possibility of using a high concentration of dopants, which is very important for short length optical amplifiers [11].

Among the RE ions, trivalent dysprosium (Dy^{3+})-doped glasses have been considered as promising materials for 1.3 μm ($^6F_{11/2}$ ($^6H_{9/2}$) $\rightarrow {}^6H_{15/2}$) emission [12, 13] as well as for two-color phosphors since Dy^{3+} ion possess strong emission at around blue (at around 486 nm, $^4F_{9/2} \rightarrow {}^6H_{15/2}$) and yellow (at around 575 nm, $^4F_{9/2} \rightarrow {}^6H_{13/2}$) colors [14–16]. Further, it is well known that the $^4F_{9/2} \rightarrow {}^6H_{13/2}$ transition of Dy^{3+} ions is hypersensitive and therefore its intensity strongly dependent on the nature of the host, whereas the intensity of magnetic-dipole allowed $^4F_{9/2} \rightarrow {}^6H_{15/2}$ transition is less sensitive to the host. Hence, at a suitable environment the intensity ratio of these transitions (Y/B) will be such that the Dy^{3+}-doped materials will generate white light [14–16]. This study reports the concentration-dependent optical properties of Dy^{3+}-doped sodium–aluminum–phosphate glass (NAP) systems. Judd–Ofelt (JO) theory has been used to analyze the absorption spectral intensities of Dy^{3+} ions in NAP glass to evaluate the radiative processes of Dy^{3+} ion excited states. It is interesting to note that the white light emitting property of

---

A. Amarnath Reddy · M. Chandra Sekhar · K. Pradeesh ·
G. Vijaya Prakash (✉)
Nanophotonics Laboratory, Department of Physics, Indian
Institute of Technology Delhi, New Delhi 110016, India
e-mail: prakash@physics.iitd.ac.in

S. Surendra Babu
Laser Instrumentation Design Centre, Instrument Research and
Development Establishment, Raipur Road, Dehradun 248008,
India

Dy^{3+}-doped NAP glass changes as a function of Dy_2O_3 concentration and excitation wavelength.

Experimental details

Dy^{3+}-doped $Na_3Al_2P_3O_{12}$ (NAP) glasses in the form of 92NAP-$(8 - x)Al_2O_3$-$(x)Dy_2O_3$ (where $x = 1$–5) were prepared using the melt quenching technique. $(NH_4)_2HPO_4$, $NaNO_3$, Al_2O_3, and Dy_2O_3 (Analytical grade) (Aldrich Chemical Co., USA) were taken as starting materials. About 10 g of batch compositions was taken in an agate mortar and was mixed and ground thoroughly using spectroscopic grade iso-proponal. Then the mixture was taken in a porcelain crucible and is placed in an electric furnace. The temperature was raised slowly to 300 °C and was maintained for about an hour and then slowly increased up to 600 °C, to ensure a complete decomposition of $(NH_4)_2HPO_4$ into P_2O_5. Subsequently the temperature of the mixture was raised to 1280 °C to get a clear melt and was maintained at that temperature for an hour. The melt was poured onto a preheated brass mold and annealed at 350 °C for about 24 h to remove the thermal strains. Then the glass samples were allowed to cool to the room temperature and were polished for optical measurements. The glass samples were polished to the commercial quality using a water-free lubricant. For more than 5 wt% of Dy_2O_3 concentration, the glass has resulted into opaque in nature.

The absorption spectra of Dy^{3+}-doped NAP glasses were recorded using a Perkin-Elmer UV–Vis–NIR spectrophotometer. 410 nm of a diode laser was used as excitations source for both luminescence emission and decay time measurements. The emitted signal was dispersed by a monochromator (Acton SP2300), and observed with a Photo Multiplier Tube (PMT) and a Si detector (PMT; Acton SP2300) which are interfaced with a computer. Decay curves were obtained using a digital storage oscilloscope (Tektronix TDS1001B) interfaced to a personal computer that records and averages the signal. Refractive index (RI) measurements for glasses were carried out by Brewster angle setup consisting of He–Ne laser (632 nm) and a Si-detector.

Results and discussion

Physical properties

Important physical and optical parameters such as RI (n), density (ρ), molar RI (R_m), molar volume (V_m), optical band gap (E_{opt}), and Urbach energies (ΔE) for the Dy^{3+}-doped NAP glasses were determined from the experimental data and are listed in Table 1. Optical band gap of the Dy^{3+}-doped NAP glass has been estimated from the absorption spectra and the values are found to be in the range of 3.33–3.38 eV. The width of localized states within the optical band gap, known as Urbach energies (ΔE), was also estimated from the absorption spectra. These ΔE values are found to be in the range between 0.29 and 0.35 eV which are close to those obtained for the other phosphate glasses [17–19]. Such lower values suggest the presence of minimum defects in the NAP glass system. RI values of RE-doped NAP glasses show an increasing trend with the increase in RE ion concentration, except for the 5 wt% Dy_2O_3-doped glass. In general, in oxide glasses the ionic refractivity of non-bridging oxygens is larger than that of bridging oxygens [20]. Compared to crystalline NASICON, $K_3Al_2P_3O_{12}$ glass [21], the structure of NAP ($Na_3Al_2P_3O_{12}$) glass can be visualized as an anionic framework built from corner-shared tetrahedral coordination of AlO_4 and PO_4 networks, where PO_4 tetrahedra pointing their unshared oxygen atoms toward the channels occupied by alkali (Na or K) ions. Therefore, this type of structure could possibly increase the number of non-bridging oxygen [22], while Al^{3+} ions were compensated by the RE ions, which could be one of the possible reasons for the increase in RI values.

Optical properties of Dy^{3+}-doped NAP glass

The optical absorption spectra for various wt% of Dy_2O_3-doped NAP glasses have been recorded in the wavelength range of 350–2000 nm. The representative absorption spectrum of 2 wt% Dy_2O_3-doped NAP glass is shown in Fig. 1. The absorption spectra of NAP glasses doped with

Table 1 Physical and optical properties of Dy^{3+}-doped NAP glasses

Property	NAP:Dy (wt%)				
	1	2	3	4	5
E_{opt} (±0.01 eV)	3.34	3.38	3.36	3.33	3.37
Urbach ΔE (±0.01 eV)	0.28	0.29	0.29	0.35	0.30
Glass thickness (±0.01 mm)	3.51	4.01	3.28	3.81	3.36
RI (±0.005)	1.530	1.545	1.564	1.572	1.560
Density ρ (g/cm^3)	2.56	2.58	2.61	2.64	2.63
Molecular weight M (g/mol)	329.75	330.16	330.52	332.04	332.28
Molar volume V_m (cm^3/mol)	128.80	127.96	126.63	125.77	126.34
Molar refraction R_m (cm^3/mol)	39.85	40.46	41.18	40.98	40.85
Reflection loss (%)	4.38	4.58	4.83	4.94	4.78
Polarizability α (Å^3)	15.80	16.04	16.33	16.41	16.20

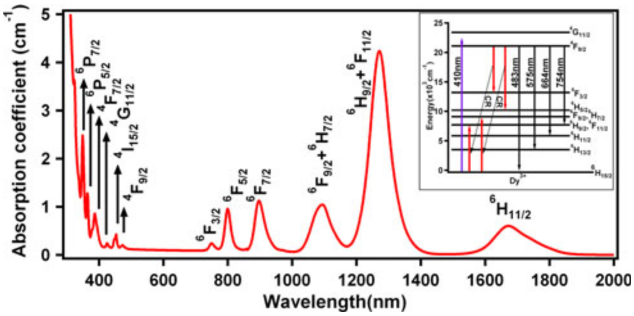

Fig. 1 Absorption spectrum of 2 wt% Dy_2O_3-doped NAP glasses. *Inset* shows the partial energy level diagram of Dy^{3+} ions in NAP glass

other wt% are also similar, except a change in the optical densities and peak intensities, and are similar to other reported glass systems [12–16, 23, 24]. As can be seen from the figure, the spectrum consists of several inhomogeneous broadened *f–f* transitions that originate from the $4f^9$ configuration of Dy^{3+} ions. These absorption bands correspond to the absorption transitions from ground $^6H_{15/2}$ state to various excited states of Dy^{3+} ion. The measured absorption spectrum of 1 wt% of Dy_2O_3 in NAP glass has been used for JO analysis. The oscillator strengths (f_{exp}) of various *f–f* transitions were evaluated and are used in the frame work of JO theory [25, 26]. A least-square fitting approximation is adopted to determine the JO intensity parameters, which gives the best-fit between the experimental and calculated oscillator strengths. The experimental and theoretical oscillator strengths obtained from JO theory are listed in Table 2 along with the experimental oscillator strengths of other reported Dy^{3+}-doped glass systems. In the present JO analysis the absorption levels lying at lower wavelength are neglected as there exist an uncertainty in finding the f_{exp} due to overlap of the levels. As can be seen from the table, the oscillator strengths of various absorption transitions are well within the range of their common occurrence.

The phenomenological JO parameters for Dy^{3+} ions in NAP glass are found to be $\Omega_2 = 6.68 \pm 0.02 \times 10^{-20}$ cm^2, $\Omega_4 = 1.10 \pm 0.025 \times 10^{-20}$ cm^2, $\Omega_6 = 1.73 \pm 0.015 \times 10^{-20}$ cm^2. These JO parameters are comparable to the other phosphate and fluorophosphates glasses [23, 24] and are more than the fluoride glasses [12, 14] reported earlier. In general, the position and oscillator strengths of absorption transitions are sensitive to the local environment of RE ion sites occupied within the glass network [27]. Therefore, these parameters provide critical information on the nature of bond between RE ions to the surrounding ligands. Among these three, Ω_2 is most sensitive to local structure and to host composition. It is known that Ω_2 increases with increase in covalence [28]. Relatively larger Ω_2 value indicates that the Dy–O bond in NAP glasses is predominantly of covalent in nature [23], where as the ionic nature of Dy–ligand bond in fluoride glasses is clearly reflected by the lower Ω_2 value [12, 14].

The JO parameters determined from the absorption spectra are used along with RI to predict the important radiative properties such as transition probabilities, branching ratios, and radiative lifetimes for the excited states of Dy^{3+} ions. The radiative transition probability (A) for a transition can be calculated from the following equation

$$A = \frac{64\pi^4 e^2}{3h(2J+1)\lambda}\frac{n(n^2+2)^2}{9}\sum_{\lambda=2,4,6}\Omega_\lambda\left|\left\langle \Psi J\middle\|U^{(\lambda)}\middle\|\Psi' J'\right\rangle\right|^2 \tag{1}$$

The total radiative transition probability (A_{T}) involving all the transitions from an excited state to lower states is given by the sum of transition probability ($A_{\mathrm{T}} = \Sigma A$). The predicted radiative lifetime (τ_{R}) of an excited state in terms of

Table 2 Experimental (*f*exp) and calculated (*f*cal) oscillator strengths ($\times 10^{-6}$) of Dy^{3+} ions in NAP glass and other Dy^{3+}-doped glasses

Transition from $^6H_{15/2}$	Energy (cm^{-1})	Dy:NAP		Lead borate [14]		PKBAD [23]		PKMAFDy [24]	
		Expt	Cal	Expt	Cal	Expt	Cal	Expt	Cal
$6H_{11/2}$	5988	0.749	0.977	1.29	1.37	0.88	1.18	0.96	0.93
$^6H_{9/2} + ^6F_{11/2}$	7868	5.534	5.518	5.73	5.71	9.12	9.08	6.02	6.02
$^6F_{9/2} + ^6H_{7/2}$	9141	1.572	1.608	2.33	2.35	2.45	2.59	2.09	1.78
$^6F_{7/2}$	11161	1.513	1.437	2.33	2.26	2.07	1.67	0.93	1.38
$^6F_{5/2}$	12531	0.780	0.694	1.37	1.12	1.14	0.67	0.69	0.62
$^6F_{3/2}$	13333	0.123	0.131	0.22	0.21	0.21	0.13	0.12	0.11
$^4F_{9/2}$	21092	0.142	0.113	0.26	0.18	0.17	0.13	0.07	0.11
$^4I_{15/2}$	22075	0.359	0.331	0.44	0.49	0.68	0.39	0.34	0.32
$^4G_{11/2}$	23529	0.087	0.036	0.18	0.05	0.09	0.11	0.12	0.06
RMS		±0.08		±0.70		±0.42		±0.44	

A_T, the total radiative transition probability of an excited state, is given by $\tau_R = 1/A_T$. The A_T is found to be 903 s^{-1} which gives a τ_R value of 1.107 ms for 1 wt% Dy^{3+}-doped NAP glass. This τ_R value is found to be higher than that found in other glasses [12–16, 23, 24].

Emission spectra

Visible emission spectra of Dy^{3+}-doped NAP glasses are shown in Fig. 2a for various Dy^{3+} ion concentrations. Since the excitation energies of 410 nm are greater than $^4F_{9/2}$ levels, the excess energy is lost in the form of phonon energy through non-radiative channels and populates the $^4F_{9/2}$ level. These emission spectra corresponds to $^4F_{9/2} \rightarrow {}^6H_J$ ($J = 9/2$, 11/2, 13/2, and 15/2) transitions of Dy^{3+} ions in the NAP glasses. As can be seen from the spectra, the emission transitions are broad, because of the availability of large number of Stark levels for $^4F_{9/2}$ and ^6H_J levels and non-removal of degeneracy of these levels. Among $^4F_{9/2} \rightarrow {}^6H_J$ transitions, the blue ($^4F_{9/2} \rightarrow {}^6H_{15/2}$) at ~485 nm and yellow ($^4F_{9/2} \rightarrow {}^6H_{13/2}$) at ~575 nm emission transitions are relatively more intense than the other emission transitions ($^4F_{9/2} \rightarrow {}^6H_{11/2,\ 9/2}$) observed in the red and near infrared regions as shown in Fig. 2a. Several spectral parameters (concentration, λ, $\Delta\lambda$, emission cross section, and τ_{exp}) for Dy^{3+} ions in NAP glasses were evaluated from the luminescence measurements. The results are given in Table 3. From the experimental emission spectra, the stimulated emission cross sections, $\sigma(\lambda_p)$, of the blue and yellow emissions were evaluated using the following equation:

$$\sigma(\lambda_p) = \frac{\lambda_p^4 A}{8\pi c n^2 \Delta\lambda_{eff}} \quad (2)$$

where λ_p is the emission peak wavelength and $\Delta\lambda_{eff}$ is the emission effective linewidth of the transition given by

$$\Delta\lambda_{eff} = \frac{1}{I_p}\int I(\lambda)d\lambda. \quad (3)$$

The observed λ_p, $\sigma(\lambda_p)$, and $\Delta\lambda_{eff}$ values of these two transitions were listed in Table 3. As can be seen from the table, all these parameters are well within the range of commonly reported values for Dy^{3+}-doped glass systems.

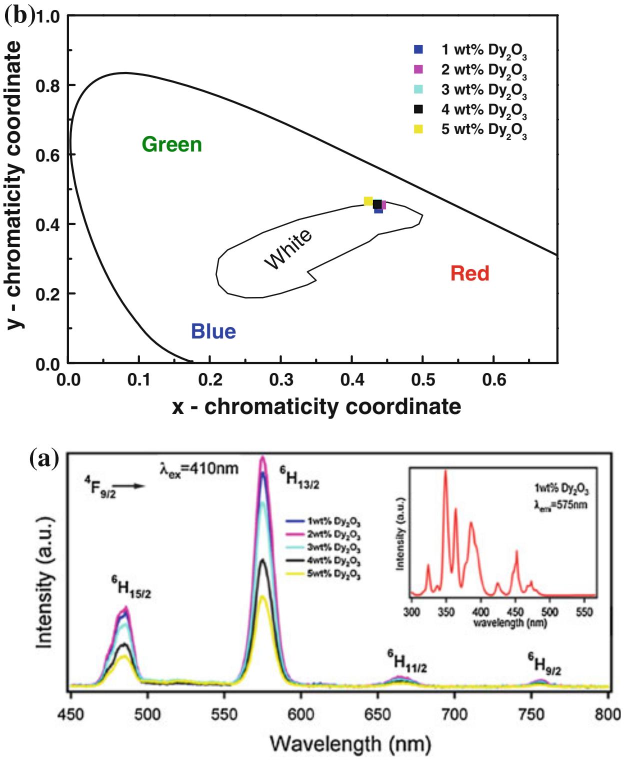

Fig. 2 **a** Emission spectra of various wt% Dy_2O_3-doped NAP glasses. The *inset* shows the excitation spectra of 575 nm emission of 1 wt% Dy_2O_3-doped NAP glass. **b** CIE coordinate diagram of various Dy^{3+}-doped NAP gasses by 410 nm excitation

The inset of Fig. 2a exemplifies the excitation spectrum of Dy^{3+} ions in NAP glasses (1 wt%), with emission at $\lambda = 575$ nm of $^4F_{9/2} \rightarrow {}^6H_{13/2}$. As can be seen from the inset there are several excitation bands situating between 300 and 500 nm, suggesting the suitable wavelength to excite the Dy^{3+} ions with UV or violet/blue lasers. It is well known that the $^4F_{9/2} \rightarrow {}^6H_{13/2}$ transition is hypersensitive ($\Delta L = 2$ and $\Delta J = 2$) and therefore, its intensity strongly depends on the host, whereas intensity of the $^4F_{9/2} \rightarrow {}^6H_{15/2}$ transition is less sensitive to the host. The Y/B ratios of all the Dy^{3+}-doped NAP glasses are in the range 2.90–3.12 (Table 4). These Y/B ratios are comparable to those obtained for Dy^{3+}-doped silicate [12] and borate [29] glasses, but considerably higher than those obtained for other phosphate glasses [16]. Even though the emission intensity decreases with the increase in concentration, the Y/B ratio is nearly equal for all the Dy^{3+}-doped NAP glasses suggesting that the local environment around Dy^{3+} is invariant with varying concentration. Comparatively larger Y/B ratios suggest the pronounced nature of covalency and asymmetry effects [10]. These Y/B intensity ratios of visible emission indicate the feasibility of generation of white light in the Dy^{3+}-doped NAP glass. The chromaticity color coordinates for Dy^{3+}-doped NAP glasses with various concentration of Dy_2O_3 wt% were calculated and shown in Table 4, and the corresponding CIE *x*–*y* chromaticity diagram are also presented in Fig. 2b. The CIE coordinates of all investigated glasses, excited with 410 nm, lies within the white region, though they are far away from the ideal equal energy white light illumination (0.333, 0.333) and there exists a tendency to be away from it with increasing Dy^{3+} ion concentrations. Further studies on simulation of white light for these Dy^{3+}-doped NAP glasses are necessary by both adjusting the glass compositions and enhancing the red emission part by co-doping.

Table 3 Concentration of Dy^{3+} ions and spectroscopic properties (λ, $\Delta\lambda$, emission cross section, and τ_{exp}) of Dy^{3+}-doped NAP glasses

Dy (wt%)	Concentration ($\times 10^{20}$ ion/cm^3)	Effective line width (nm ±0.05)		Emission cross section ($\times 10^{-21}$ cm^2)		Life time $^4F_{9/2} \rightarrow {}^6H_{13/2}$ (±0.01 ms)
		484 nm	575 nm	484 nm	575 nm	
1	0.95	15.71	14.33	0.42	3.58	1.03
2	1.91	15.60	14.45	0.43	3.68	0.63
3	2.90	15.40	14.33	0.44	3.74	0.53
4	3.91	15.24	14.32	0.44	3.78	0.39
5	4.86	15.30	14.26	0.43	3.71	0.40

Table 4 Yellow to blue intensity ratios and chromaticity color co-ordinates of various concentration of Dy^{3+}-doped NAP glasses under 410 nm excitation

Dy^{3+} concentration (wt%)	Y/B	Color coordinates	
		x	*y*
1	2.90	0.438	0.443
2	2.92	0.442	0.454
3	2.99	0.437	0.459
4	3.02	0.436	0.456
5	3.12	0.424	0.465

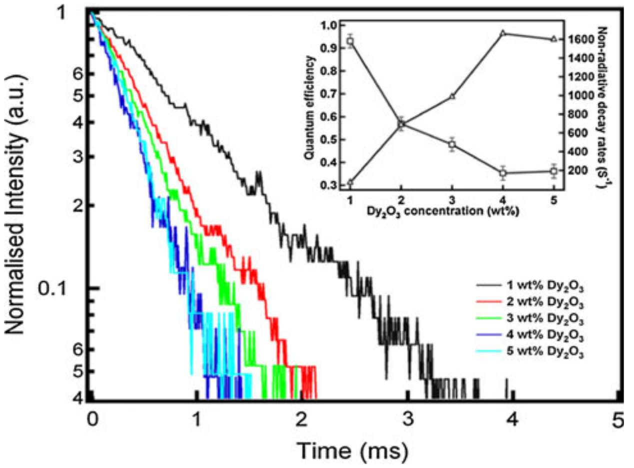

Fig. 3 Decay curves of $^4F_{9/2}$ level monitored at $^4F_{9/2} \rightarrow {}^6H_{13/2}$ transition in various wt% Dy_2O_3-doped NAP glasses. *Inset* shows the variation of quantum efficiency and non-radiative decay rate of $^4F_{9/2}$ level with Dy_2O_3 concentration

Decay time measurements

Figure 3 shows the luminescence decay curves of the intense luminescent $^4F_{9/2} \rightarrow {}^6H_{13/2}$ transition for some of the Dy^{3+}:NAP glasses. It is interesting to note that the decay curves are almost single exponential even for higher Dy^{3+} ion concentrations. All the normalized experimental decay curves are fitted with the function $y(t) = A\exp(-t/\tau)$, where τ is the emission life time. The exponential nature of the decay curves is due to either fast decay of excited Dy^{3+} ions or the effect of ligands is considerably small on Dy^{3+} ions [30]. The lifetime values of $^4F_{9/2}$ level are tabulated in Table 3. It is clear from the table that the lifetime decreases with increase in the concentration of Dy^{3+} ions. The experimental lifetime of $^4F_{9/2}$ level in Dy^{3+}:NAP glasses is found to be higher than other phosphate, borate, lead borate glasses [14, 23, 24, 29] and lower than the fluorophosphates glasses [31].

The luminescence quantum efficiency (η) is defined as the ratio of the number of photons emitted to the number of photons absorbed. For RE ion systems it is equal to the ratio of the measured lifetime to the predicted radiative lifetime for respective levels given by $\eta = \tau_{exp}/\tau_R$. The non-radiative decay rate (W_{nr}) is given by $W_{nr} = \frac{1}{\tau_{exp}} - (A_T)$ where (A_T) is the total radiative transition probability determined through JO analysis. The η for $^4F_{9/2}$ level in 1 wt% Dy_2O_3-doped NAP glass is found to be 93%, which is higher than other reported glasses. The inset of Fig. 3 shows the variations of η and W_{nr} with Dy_2O_3 concentration. As can be seen from the inset, W_{nr} increases and η decreases with increase in Dy_2O_3 concentration. The considerably increasing value of W_{nr} indicates the presence of non-radiative channel in the relaxation of $^4F_{9/2}$ level. As the concentration of RE ion is increased, the RE ions tend to form clustering and as a consequence the emission lifetime of the RE ions are reduced [32]. The other quenching mechanisms responsible for the reduction of lifetime with increase in concentration could be up-conversion and cross relaxation. As the maximum phonon energy of phosphate is large enough to neglect the up-conversion effects in the present case. Hence, the decrease in the lifetime may be due to cross relaxation between Dy^{3+} ions with increase in concentration from 2 to 5 wt%. Different cross-relaxation processes that can account for this energy transfer between Dy^{3+} ions in the NAP glasses may be $^4F_{9/2} + {}^6H_{15/2} \rightarrow {}^6H_{5/2} + {}^6H_{7/2}$ and $^4F_{9/2} + {}^6H_{15/2} \rightarrow {}^6F_{3/2} + ({}^6H_{9/2}, {}^6F_{11/2})$. The inset of Fig. 1 shows the possible cross-relaxation channels. This kind of cross relaxation is also observed in other glasses including lead borate [14], borate [29], and phosphate [23, 24] glasses.

Conclusions

A new class of dysprosium-doped glasses with compositions 92NAP–(8 − x)Al_2O_3–(x)RE_2O_3 (where x =1–5 wt%) was prepared and characterized. The optical properties, viz., RI, optical bandgap, absorption and photoluminescence and decay times Dy^{3+} ions were studied and related to the host matrix nature. The absorption spectra are analyzed using the JO theory, from the integrated intensities of various absorption bands. The JO parameter Ω_2 value indicates that these doped glasses are more covalent in nature. Strong yellow and blue emissions were observed upon the 410 nm excitation wavelengths. The emission intensity ratios of yellow and blue transitions, Y/B, of Dy^{3+} ions indicate the strong covalent nature and dependence on the local environment in which the RE ions are occupied. These results also show the possibility of obtaining white light from the titled glasses. These Na-based phosphate glasses are highly transparent and capable to accommodate larger concentrations of RE ions; therefore, these glasses are of particular interest for developing ion-exchange waveguide-based devices and suitable for white light generation.

Acknowledgement One of the authors (G.V.P.) acknowledges the financial support from Department of Information Technology (DIT), Govt. of India, under Photonics Development Program (ref: 12(1)/2008-PDD).

References

1. Optical technologies in motion, European commission's Information society technologies (IST-OPTIMIST), Fifth framework (FP-5, 1998–2002) projects. www.ist-optimist.org
2. Yamada M, Shimizu M (2003) Nippon Telegraph Telephone Corporation (NTT) Technical Rev 1(3):80. www.ntt.co.jp
3. Aozasa S et al (2004) Nippon Telegraph Telephone Corporation (NTT) Technical Rev 2(12):44. www.ntt.co.jp
4. Wagener JL, Hodgson CW, Digonnet MJF, Shaw HJ (1997) J Lightw Technol 15:1681
5. Vijaya Prakash G (2000) Mater Lett 46:15 and references therein
6. Mariappan CR, Govindaraj G, Rathan SV, Vijaya Prakash G (2005) Mater Sci Eng B 123:63
7. Mariappan CR, Govindaraj G, Rathan SV, Vijaya Prakash G (2005) Mater Sci Eng B 121:2
8. Vijaya Prakash G, Jagannathan R (1999) Spectrochim Acta A 55:1799 and references therein
9. Brow RK, Kirkpatrick RJ, Turner GL (1993) J Am Ceram Soc 76:919
10. Seneschal K, Smektala F, Jiang S, Luo T, Bureau B, Lucas J, Peyghambarian N (2003) J Non-Cryst Solids 324:179
11. Lakshminarayana G, Qiu J, Brik MG, Kumar GA, Kityk IV (2008) J Phys Condens Matter 20:375101
12. Duan Z, Zhang J, Hu L (2007) J Appl Phys 101:043110
13. Yang Z, Li B, He F, Luo L, Chen W (2008) J Non-Cryst Solids 354:1198
14. Pisarska J (2009) J Phys Condens Matter 21:285101
15. Sun X, Huang S, Gong X, Gao Q, Ye Z, Cao C (2010) J Non-Cryst Solids 356:98
16. Jayasimhadri M, Jang K, Lee HS, Chen B, Yi S-S, Jeong J-H (2009) J Appl Phys 106:013105
17. Pradeesh K, Otton CJ, Agotiya VK, Raghavendra M, Vijaya Prakash G (2008) Opt Mater 31:155
18. Subrahmanyam K, Salagram M (2000) Opt Mater 15:181
19. Gray P (1984) J Non-Cryst Solids 68:75
20. Kingery WD, Bowen HK, Uhlmann DR (1976) Introduction to ceramics. Wiley, New York
21. Nandini Devi R, Vidyasagar K (2000) Inorg Chem 39:2391
22. Jiang S, Luo T, Hwang B-C, Smekatala F, Seneschal K, Lucas J, Peyghambarian N (2000) J Non-Cryst Solids 263:364
23. Surendra Babu S, Babu P, Jayasankar CK, Troster Th, Sievers W, Wortmann G (2009) Opt Mater 31:624
24. Basavapoornima Ch, Jayasankar CK, Chandrachoodan PP (2009) Physica B 404:235
25. Judd BR (1962) Phys Rev 127:750
26. Ofelt GS (1962) J Chem Phys 37:511
27. Reisfeld R, Jorgensen CK (1975) Lasers and excited states of rare-earths. Springer Verlag, New York
28. Jayasimhadri M, Moorthy LR, Kojima K, Yamamoto K, Wada N (2006) J Phys D Appl Phys 39:635
29. Jayasankar CK, Venkatramu V, Surendra Babu S, Babu P (2004) J Alloys Compd 374:22
30. Azkargorta J, Iparraguirre I, Balda R, Fernandez J, Denoue E, Adam JL (1994) J IEEE Quantum Electron 30:1862
31. Herrmann A, Ehrtn D (2008) J Non-Cryst Solids 354:916
32. Zhiwu P, Qiang S, Yongsheng C, Jlyu Z (1991) Mater Res Bull 26:1059